

RESEARCH ARTICLE

The anterior nucleus of the thalamus plays a role in the epileptic network

Hao Yan^{1,a} , Xueyuan Wang^{1,a} , Tao Yu^{1,b} , Duanyu Ni¹, Liang Qiao¹, Xiaohua Zhang¹, Cuiping Xu¹, Wei Shu¹, Yuping Wang² & Liankun Ren^{2,b} 

¹Department of Functional Neurosurgery, Beijing Institute of Functional Neurosurgery, Xuanwu Hospital, Capital Medical University, Beijing, China
²Department of Neurology, Comprehensive Epilepsy Center of Beijing, Beijing Key Laboratory of Neuromodulation, Xuanwu Hospital, Capital Medical University, Beijing, China

Correspondence

Tao Yu, Beijing Institute of Functional Neurosurgery, Department of Functional Neurosurgery, Xuanwu Hospital Capital Medical University, Beijing 100053, China. Tel: +86 10 83198671; Fax: +86 10 83163174; E-mail: yutaoly@sina.com
Liankun Ren, Department of Neurology, Xuanwu Hospital, Capital Medical University, 45 Changchun Street, 100053 Beijing, China. Tel: +86 10 83198273; Fax: +86 10 83157841; E-mail: rlkbrain2000@yahoo.com

Funding Information

This study is supported by the Beijing Natural Science Foundation of China-Beijing Municipal Education Commission Joint Fund (KZ202110025036); Science and Technology Innovation Project (2021ZD0201605); Beijing Natural Science Foundation (Z210009).

Received: 17 August 2022; Revised: 10 October 2022; Accepted: 24 October 2022

Annals of Clinical and Translational Neurology 2022; 9(12): 2010–2024

doi: 10.1002/acn3.51693

^aCo-first authors.

^bCo-corresponding authors.

Introduction

Over the last few decades, deep brain stimulation (DBS) has emerged as a viable therapy for drug-resistant epilepsy.^{1,2} Several potential brain targets have been investigated for the treatment of drug-resistant epilepsy.^{3–6} The anterior nucleus of the thalamus (ANT) is a crucial relaying node in the Papez circuitry and a critical nucleus in the intra-thalamic pathways.⁷ Therefore, ANT is considered a promising target for DBS to treat medically drug-

Abstract

Objectives: We investigated both the metabolic differences and interictal/ictal discharges of the anterior nucleus of the thalamus (ANT) in patients with epilepsy to clarify the relationship between the ANT and the epileptic network. **Methods:** Nineteen patients with drug-resistant epilepsy who underwent stereo-electroencephalography were studied. Metabolic differences in ANT were analyzed using [18F] fluorodeoxyglucose–positron emission tomography with three-dimensional (3D) visual and quantitative analyses. Interictal and ictal discharges in the ANT were analyzed using visual and time-frequency analyses. The relationship between interictal discharge and metabolic differences was analyzed. **Results:** We found that patients with temporal lobe epilepsy (TLE) showed significant metabolic differences in bilateral ANT compared with extratemporal lobe epilepsy in 3D visual and quantitative analyses. Four types of interictal activities were recorded from the ANT: spike, high-frequency oscillation (HFO), slow-wave, and α -rhythmic activity. Spike and HFO waveforms were recorded mainly in patients with TLE. Two spike patterns were recorded: synchronous and independent. In 83.3% of patients, ANT was involved during seizures. Three seizure onset types of ANT were recorded: low-voltage fast activity, rhythmic spikes, and theta band discharge. The time interval of seizure onset between the seizure onset zone and ANT showed two patterns: immediate and delayed. **Interpretation:** ANT can receive either interictal discharges or ictal discharges which propagate from the epileptogenic zones. Independent epileptic discharges can also be recorded from the ANT in some patients. Metabolic anomalies and epileptic discharges in the ANT indicate that the ANT plays a role in the epileptic network in most patients with epilepsy, especially TLE.

resistant epilepsy, and its feasibility has been demonstrated in a series of previous studies.^{8,9} However, despite extensive research, the exact therapeutic mechanism of ANT-DBS in focal epilepsy remains unclear.¹⁰ The conception that epilepsy is a cortico-subcortical disease had been discussed as early as the 1970 s.¹¹ Several animals^{12,13} and neuroimaging^{3,14} studies demonstrated the involvement of the subcortical nuclei in the cortico-subcortical epileptic network. Although previous studies have also demonstrated the participation of the ANT in

the propagation of epileptic seizures,^{12,15–18} a particularly pertinent unanswered question is whether the ANT acts solely as an important node in ictal propagation, or, no matter during the interictal or ictal stage, it plays roles in the cortical–subcortical epileptic network. Existing but limited studies support the latter hypothesis.¹⁶

During pre-surgical evaluations, we observed metabolic differences in [18F] fluorodeoxyglucose-positron emission tomography (FDG-PET) in the bilateral ANT in some patients with focal epilepsy. Interestingly, the hypometabolism of FDG-PET usually includes the epileptogenic zone or occurs in closely related cortical regions in patients with focal epilepsy.^{19,20} Why does ANT exhibit focal hypometabolism? Revealing the causes of hypometabolism in ANT in patients with epilepsy may help us identify the precise role of ANT in epileptic networks.

In principle, gaining an increased understanding of the electrophysiological properties of the ANT and the electrophysiological relationship between the ANT and the epileptogenic zone may help identify the mechanism responsible for hypometabolism in the ANT in patients with focal epilepsy. Here, we describe the results of FDG-PET and direct stereoelectroencephalography (SEEG) recordings of the ANT in patients with drug-resistant focal epilepsy. In this way, we attempted to identify the potential relationship between ANT and epileptic networks. Our findings will be helpful in deepening our understanding of the mechanisms of ANT-DBS.

Methods

Clinical population

All participants were patients with drug-resistant epilepsy who were admitted for consultation at the Beijing Institute of Functional Neurosurgery, Xuanwu Hospital, between January 2018 and December 2019. All patients were diagnosed with drug-resistant epilepsy according to the ILAE Classification of Epilepsies and received a presurgical evaluation for epilepsy surgery.²¹

Standard protocol approvals, registrations and patient consent

The ethics committee of the Capital Medical University approved this study (Reference: LYS2018041), and written informed consent was obtained from all included patients.

Presurgical evaluation

Each patient underwent interictal/ictal scalp electroencephalography (EEG) recordings using a video-EEG

monitoring system (Micromed, Treviso, Italy), with electrodes placed according to the international 10–20 system. The duration of video EEG monitoring ranged from 3 to 14 days, and at least three habitual seizures were recorded for each patient. All information acquired by interictal and ictal EEG, along with the symptomatic characteristics of each patient, were analysed to assist in locating the epileptogenic zones (EZs).

All patients underwent a high-resolution magnetic resonance imaging (MRI) protocol that was performed using a 3.0-T MR Scanner (Siemens, Verio, Germany) and consisted of conventional spin-echo T1-weighted axial, sagittal, coronal and T2-weighted axial sequences (section thickness of 5 mm, image gaps of 1 mm). In addition, fluid-attenuated inversion recovery images were obtained with a thickness of 5 mm. We also acquired three-dimensional anatomical T1-weighted axial, sagittal and coronal sequences covering the whole-brain volume with a 1-mm section thickness.

18F-fluorodeoxyglucose (18F-FDG) Positron Emission Tomography (PET) was also performed on all patients to facilitate the localization of the EZs. The interictal PET scanner had an isotropic spatial resolution of 5 mm and generated images with a slice thickness of 2.44 mm. Similar to the process of post-surgical CT, the PET image was co-registered with the T1 image in the same space, and the contrast and colour table was adjusted with an optional threshold.

The localization of EZs, as well as the relationship between the EZs and the functional cortex, was fully evaluated by a special committee when the clinical data were collected. According to the committee, SEEG electrodes were needed due to a lack of sufficient information arising from non-invasive studies performed on these patients. A common trait among these patients was that we used electrodes to explore the opercula-insular cortex or the inferior/middle frontal lobe.

The implantation, reconstruction and localization of the SEEG electrode

The SEEG electrodes were implanted using intra-cerebral multiple-contact electrodes (10–16 contacts; length, 2 mm; diameter, 0.8 mm. 1.5-mm apart) that were placed intra-cerebrally according to the stereotactic method and facilitated using a robotic arm-assisted system (Sinovation Medical Technology, Beijing, China). The plan was discussed and designed by experienced neurologists and neurosurgeons. The number of SEEG electrodes and anatomical targeting were designed based on the information provided by the evaluation of non-invasive localization and the proposed hypothesis for localization. SEEG electrodes were used to investigate the opercula-insular

cortex or inferior/middle frontal lobe and were adjusted subtly so that their tips could enter the ANT. Post-surgical CT scans were performed to verify the locations of the contacts and to identify post-operative complications.

The reconstruction and localization of the depth electrodes were performed in accordance with established protocols.²² In brief, based on MRI before implantation, we used the FreeSurfer image analysis suite (<https://surfer.nmr.mgh.harvard.edu/>) to reconstruct the cortical surface. The post-operative CT image was then co-registered with the T1 image and converted into Talairach space. Electrodes were detected using clustering-based segmentation. The direction, starting point and deepest point of the electrodes were verified using the pre-surgical designation. The trajectory of each electrode was fitted to a curve, and the contacts were represented by equally spaced dots.

Quantitative analyses of the region of interest (ROI) and the creation of a three-dimensional (3D) ANT using PET data

The ROI of the ANT was delineated based on the Morel Stereotactic Atlas. The precise border of the ANT in each patient was adjusted subtly using different views and identified by three experienced neurosurgeons. In brief, a thin-slice scan was performed on T1 MRI sequences using a 3.0-T MRI system. This allows the mammillothalamic tract to be presented clearly, thus helping to define the ANT border indirectly.^{23,24} The choroid plexus and thalamostriate veins on the ANT surface were excluded from the ROI. To avoid the influence of hypometabolism at the margin of the lateral ventricle, the ROI boundary was reduced by 1–2 voxels compared with that of the T1 image. The ROI of the ANT was labelled with a value and saved as a label map file. We then labelled the ANT ROI on both sides. We then used the label statistics module of the 3D Slicer software (www.slicer.org) to perform data processing. Thus, we obtained the radioactivity concentration value (RCV) of the bilateral ANT ROI area, including the maximum, minimum, average, standard deviation (SD) and volume of the ROI.²⁵ RCV was assessed individually for the left and right ANT. Next, the ANT RCV was divided by the mean cerebellum RCV (“nRCV”) to facilitate comparison and reduce the variance between patients.^{26,27} The absolute asymmetry index (AAI) of each patient was calculated using Equation (1):

$$AAI = |LA - RA| \times 100 / [(LA + RA) / 2] \quad (1)$$

In Equation (1), LA indicates the mean concentration of the PET tracer in the left ANT and RA represents the mean concentration of the PET tracer in the right ANT.

Subsequently, we created a 3D model of the ANT based on the ROI. The probe volume module of the 3D Slicer was then used to project the PET data onto the surface of the ANT model. A ColdToHotRainbow colour table was used to visualize the results. The visual evaluation of metabolism in the ANT was performed by three radiologists.

SEEG recording and montage selection

Local field potentials were recorded using a 128-channel Micromed EEG acquisition system (Micromed; Treviso, Italy) and sampled at 1024 Hz. Intra-cranial electroencephalography (iEEG) data (time interval calculating and discharge counting) were analysed using the AnyWave software (<https://meg.univ-amu.fr/wiki/AnyWave/>). To reduce volume conduction, the SEEG data were processed using a bipolar montage. According to interictal and ictal recordings, the two contacts with the earliest spike in interictal and earliest involvement in the seizures were selected for each patient (Table 1). In addition, the top two contacts within the ANT were selected to read the ANT signals.

The interictal iEEG data recorded in the ANT while the patient was awake were selected and evaluated by three technicians with considerable experience in electrophysiology. We classified the ANT activities in the interictal period into four types: spike, high-frequency oscillation (HFO), slow-wave (δ and θ activities) and α -rhythmic. The definition of activity type in each patient was based on the frequency of activity recorded in the ANT. In brief, 30 awake stage 1-min blocks from iEEG interictal data were selected randomly. In addition, patients had no seizures for at least 30 min before and after these blocks. Three technicians with considerable experience in electrophysiology counted each type of activity during each block. The activity type of ANT was defined as the type with the highest cumulative quantity. In addition, when the cumulative quantity was similar between the two activity types, for example, activity A and activity B (at least $B > 1/2 A$), we would consider that two types of activity were recorded in the ANT.

Based on the non-invasive evaluation, the electrodes were designed to include both suspicious EZs and early spreading regions. Usually, more than one electrode is implanted into the suspicious EZs, in an attempt to arrange a sufficient number of contacts of the SEEG electrode in the EZs and the surrounding cortex. The synchronization pattern is identified according to the time interval between the beginning of the earliest spike in the SOZ and the ANT. Since the nerve conduction velocity between the cortex and thalamus is fast,^{28–32} only the time interval that is fewer than 30 msec is identified. Moreover, in a burst of

Table 1. Demographic and clinical data for the patient cohort.

Patient number	Age (years)	Epilepsy duration (years)	Epilepsy type	MR findings	PET findings	3D visual evaluation	Side of ANT		Surgery	Pathological diagnosis	Seizure outcome (LAE classification)
							hypometabolism (relative)	Contacts in SOZ			
1	31	29	TLE	negative	L-T, F	S	L	H	L-T, inferior F	FCD Ila + HS	II
2	10	9	TLE	L-Hippocampus atrophy	R-T	S	L	H	R-T, posterior T	FCD I	IV
3	18	11	ETLE	negative	L-F	N	R	Superior F	R-superior and medial F	FCD Iib	I
4	17	9	TLE	L-Frontal signal abnormality	R-T	S	R	H	R-T	T gliosis + HS	I
5	15	6	TLE	R-Parietal atrophy	R-T, P	S	R	H	R-T, TPO	SG + HS	I
6	23	8	ETLE	L-Hippocampus atrophy	R-F	S	L	Superior F	R-middle and superior F	FCD Iib	III
7	17	7	ETLE	negative	L-F, T	N	L	Middle F	L-middle and inferior F, anterior I	FCD Ila	I
8	2	2	ETLE	L-Frontal signal abnormality	L-F	N	L	SMA	L-middle and superior F, SMA	FCD Iib	I
9	13	1	ETLE	negative	L-F	N	L	Superior F	L-middle and superior F	FCD Ila	I
10	26	14	ETLE	R-Frontal heterotopia	L-T	S	L	Middle F	R-middle and superior F	FCD Ila + HGM	III
11	25	6	TLE	negative	L-T, F	S	L	H	L-T, the bottom of F	FCD Iib + HS	I
12	21	3	ETLE	negative	L-F, T	S	L	Opercula	R-I and opercula	-	II
13	17	8	TLE	negative	R-T, P	S	R	Superior T	R-T, posterior T	FCD Ila + HGM	I
14	27	13	TLE	negative	L-T	S	L	H	L-T	HS + FCD Iib	I
15	28	11	ETLE	negative	L-F, T	S	R	Superior F	L-ACC, superior F	FCD Iib	I
16	20	20	ETLE	L-Frontal signal abnormality	L-F	N	L	I	L-I and opercula	FCD Iib	I
17	38	14	TLE	negative	L-F	S	L	H	R-T + inferior F	FCD Ila+HS	IV
18	24	10	ETLE	negative	L-F	N	L	Posterior I	L-opercula and posterior I	FCD Iib	I
19	21	11	TLE	negative	L-T	S	L	H	L-TPO, H	FCD I	III

ACC, anterior cingulate cortex; ETLE, extratemporal lobe epilepsy; F, frontal; FCD, focal cortical dysplasia; H, hippocampus; HS, hippocampal sclerosis; HGM, heterotopic grey matter; I, insula; L, left; R, right; N, the metabolic difference in the bilateral ANT was not significant; S, the metabolic difference in the bilateral ANT was significant; SG, scar gyrus; SMA, supplementary motor area; T, temporal; TLE, temporal lobe epilepsy; TPO, tempo-parieto-occipital junction.

interictal discharges, only the contact with the earliest spike in the SOZ was selected for comparison with that of the corresponding spike in the ANT. The temporal relationship of the interictal epileptic discharges between the ANT and all of those in the EZ was compared, and a time interval greater than 30 msec was defined as the independent pattern. Twenty synchronous spikes (S spikes) were selected randomly from the iEEG data of patients, and the mean \pm standard deviation (SD) of the time interval of the beginning of the spike between the SOZ and ANT was estimated for each patient.

Ictal EEG data were collected and analysed by three technicians. Seizure onset of the ANT and SOZ was defined as the earliest change in the SEEG signal of a continuous rhythmic discharge, followed by clinical manifestations.³³ Patients with clinical signs that preceded EEG alteration (ANT and SOZ) were excluded. Three seizures were randomly selected from each patient (at least three were recorded per patient). With the help of normalized time-frequency analysis, the seizure onset types of ANT were defined as low-voltage fast activity (LVFA), rhythmic spikes (RS) and theta band discharge. Epileptic activity with the highest normalized power was the main discharge in ANT seizures with several frequency bands. Three seizures were selected, which were identical to those described above, to calculate the time interval of seizure onset between SOZ and ANT.

Surgical treatment and outcomes

The epileptic focus was localized by expert consultation based on the evidence provided by SEEG and non-invasive examinations. Depending on the location and extent of epileptic foci, surgical resection was performed in all patients. The patients were followed up for ≥ 1 year. Post-operative outcomes were graded according to the ILAE classification.³⁴

Statistical analysis

To examine the metabolic differences in the ANT within and between groups across different categories, we used paired-sample *t* tests and independent-sample *t* tests to compare nRCV and AAI differences. The nRCV and AAI of the ANT in the different groups were normally distributed (Shapiro–Wilk tests, $p > 0.05$). For this reason, and given the smaller sample size, we used Fisher's exact tests to compare group differences with regard to surgical outcomes (ILAE I and II vs. ILAE III–VI). The time interval of the beginning of the spike between SOZ and ANT was reported as the mean \pm SD. Statistical analyses were performed using the SPSS version 20.0 software (IBM, Armonk, NY, USA).

Data availability

Data supporting this study are available upon request. The data are not publicly available because it contains information that could compromise research participants' privacy consent.

Results

Nineteen patients were included in this study. The mean age at the time of surgery was 20.68 ± 8.05 years (range, 17–38 years). Patients had a history of epilepsy of 10.10 ± 6.45 years (range, 1–29 years). The demographic and clinical characteristics of the patients are summarized in Table 1. According to the type of resection, the 19 patients were divided into a temporal lobe epilepsy (TLE) group ($n = 9$) and an extratemporal lobe epilepsy (ETLE) group ($n = 10$). At the 12-month post-operative follow-up, 14 patients (73.7%) were completely free of epileptic seizures (12 patients, ILAE I) or only have occasional auras (2 patients, ILAE II). None of the patients experienced worsening seizures.

Visual evaluation of metabolism in the ANT

Upon 3D visual evaluation, the metabolic difference in the bilateral ANT was significant in eight of nine patients with TLE; in seven of these patients, the hypometabolic side of the ANT was ipsilateral to the EZ. In these seven patients, the observed ipsilateral temporal hypometabolism also decreased to varying degrees (Fig. 1A). Hypometabolism in the ANT was contralateral to the EZ in the remaining 2 patients with TLE. In 6 of the 10 patients with ETLE, the difference in metabolism in the bilateral ANT was not significant upon visual evaluation (Fig. 1B). In the remaining four patients with ETLE, the metabolic difference in the bilateral ANT was significant, although, in these patients, the hypometabolism in the ANT was contralateral to the EZ.

Quantitative analysis of ANT metabolism

The nRCV for the ANT on the EZ side was lower than that on the contralateral side in seven out of nine patients with TLE ($p = 0.034$). The nRCV in the contralateral ANT was lower than that on the EZ side in the remaining two patients. In 10 patients with ETLE, the nRCV of the ipsilateral ANT was lower in six patients. In the remaining four patients, the nRCV of the contralateral ANT was lower than that on the EZ side (Table 2). We found no significant difference in ANTs with a lower nRCV between patients with TLE and those with ETLE ($p = 0.33$). The AAI of the bilateral ANT in patients with

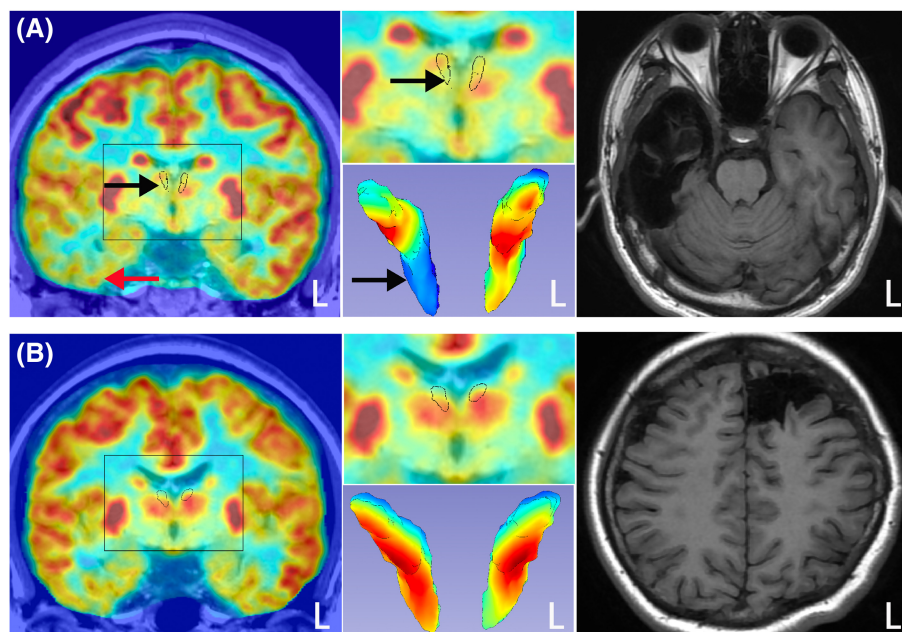


Figure 1. PET-MRI, 3D-view of the ANT and postoperative MRI in a patient with TLE (patient 5, A) and in a patient with ETLE (patient 8, B). The ANT is delineated in the coronal PET-MRI images in the left portion of (A) and (B); the middle and upper portions of (A) and (B) represent a magnified image of the ANT region; the middle and lower portions of (A) and (B) show the 3D view of the ventral side of the ANT; the right portion of (A) and (B) is the post-operative MRI. The images in (A) show hypometabolism in the temporal lobe (red arrows) and the ipsilateral ANT (black arrows). The images in (B) show that the metabolic difference in the bilateral ANT was not significant. L = left

Table 2. Quantitative analysis of metabolism in the ANT and the characteristics of epileptic discharges in the ANT

Patient number	Number of Seizures	iEEG-ANT side	L-ANT nRCV	R-ANT nRCV	AAI	Interictal activities of ANT	Time interval of S-spike (seconds)	Seizure onset type of ANT	Ictal interval pattern
1	6	L	1.51	1.68	11.04	S-spike	22.4 ± 5.6	LVFA	Immediate
2	7	R	1.27	1.37	7.38	slow-wave (3–5 Hz)	–	LVFA	Immediate
3	13	R	1.35	1.29	4.33	α-rhythmic and slow-wave (2–5 Hz)	–	None	None
4	8	R	1.11	1.03	7.12	S-spike	22.9 ± 4.6	RS	Immediate
5	5	R	1.19	1.11	6.77	S-spike	26.5 ± 4.1	RS	Immediate
6	7	R	1.18	1.27	6.96	slow-wave (1–2 Hz)	–	theta	Immediate
7	3	L	1.45	1.51	4.03	α-rhythmic and slow-wave (2–3 Hz)	–	theta	Delayed
8	22	L	1.11	1.15	3.35	slow-wave (3–5 Hz)	–	LVFA	Delayed
9	6	L	1.03	1.06	2.60	S-spike	23.1 ± 4.5	LVFA	Immediate
10	3	R	1.41	1.62	13.31	α-rhythmic and slow-wave (3–5 Hz)	–	LVFA	Immediate
11	4	L	1.41	1.66	16.20	slow-wave (3–4 Hz)	–	LVFA	Immediate
12	–	L	1.09	1.20	9.11	I-spike (rhythm)	–	None	None
13	8	R	1.35	1.22	10.25	S-spike, HFO	21.8 ± 5.0	LVFA	Immediate
14	3	L	0.94	1.06	11.75	S-spike	21.9 ± 4.1	RS	Immediate
15	12	L	1.36	1.23	9.88	I-spike	–	None	None
16	8	L	1.73	1.75	1.25	slow-wave (2–4 Hz)	–	None	None
17	11	R	1.33	1.39	4.26	S- and I-spike	21.5 ± 5.8	theta	Immediate
18	9	L	1.68	1.70	1.49	α-rhythmic and slow-wave (1–3 Hz)	–	LVFA	Delayed
19	15	L	1.36	1.60	16.31	S-spike	18.8 ± 4.8	RS	Immediate

Abbreviations: AAI, absolute asymmetry index; HFO, high-frequency oscillation; LVFA, low-voltage fast activity; RS, rhythmic spikes; L, left; R, right; S, synchronous; I, independent; nRCV, normalized radioactivity concentration.

TLE was significantly higher than in patients with ETLE (10.12 ± 4.19 vs. 5.63 ± 4.02 , $p = 0.029$). Upon exclusion of patients with hypometabolism in the ANT on the side contralateral to the epileptogenic zone, the difference was more significant (11.3 ± 3.84 vs. 3.43 ± 1.95 , $p = 0.003$) (Fig. 2A).

The electrode in the ANT was implanted ipsilaterally to the EZ in 18 patients and contralaterally to the EZ in one patient (patient 12). Hypometabolism in the ANT was ipsilateral to the EZ in 13 patients (13/19), and 12 of these 13 patients had seizure-free outcomes after surgery. In the remaining six patients with contralateral hypometabolism in the ANT, only two patients had seizure-free outcomes. Patients with contralateral ANT hypometabolism had a significantly higher risk of post-operative epilepsy than those with hypometabolism in the ANT ipsilateral to the EZ ($p = 0.017$). In patients with TLE and ETLE with ANT hypometabolism ipsilateral to the EZ, the statistical analysis showed that surgical outcomes

were not significantly different compared to patients with hypometabolism in the ANT contralateral to the EZ ($p = 0.08$, $p = 0.13$) (Fig. 2B). There was no significant correlation ($p > 0.05$) between the degree of AAI and the post-operative outcomes.

Interictal activities of the ANT

Four types of interictal activity were recorded in the 19 patients: spike, HFO, slow-wave and α -rhythmic activity. Spike was recorded in 10 patients (7 of the 10 patients had TLE). The slow-wave activity was recorded in nine patients (7 of 9 patients had ETLE). The α -rhythmic activity was recorded in four patients (4 patients had ETLE). HFO was recorded in one patient with TLE (Fig. 2 and Table 2). There were two types of activities in five patients (Figs. 3 and 4). The AAI differences between patients with spike or HFO and those with slow-wave or α -rhythmic activity were not significant ($p = 0.26$). There

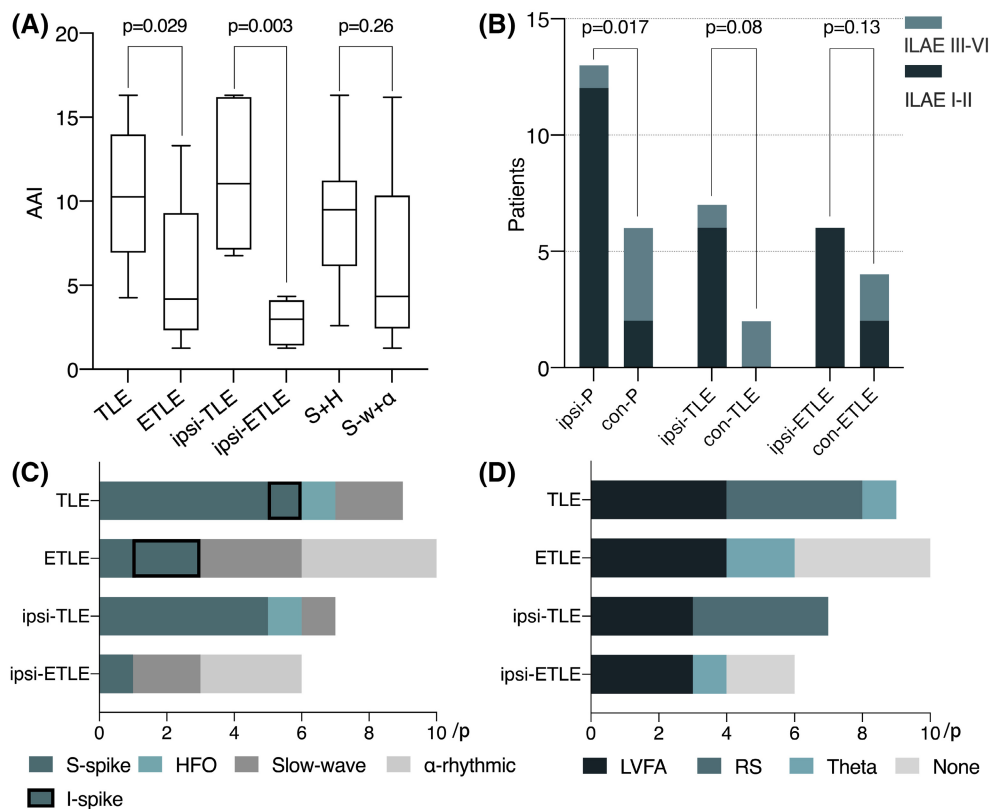


Figure 2. Differences of AAI across different categories (A) and surgical outcomes in different groups (B). (C) Distribution of the different interictal activity types in the ANT across different categories. In the group (Ipsi-) TLE, the patient with both spike and HFO is represented by HFO only, and the patient with both S spike and I spike is represented by I spike only; in the group (Ipsi-) ETLE, the patients with both α -rhythmic activities and slow-wave are represented by α -rhythmic only. (D) Distribution of the different seizure onset types in the ANT across different categories. Ipsi-, ANT hypometabolism side was ipsilateral to the EZ; con-, the ANT hypometabolism side was contralateral to the EZ; P, all patients; S + H, patients with spike and HFO; S - w + α , patients with slow-wave and α -rhythmic activity.

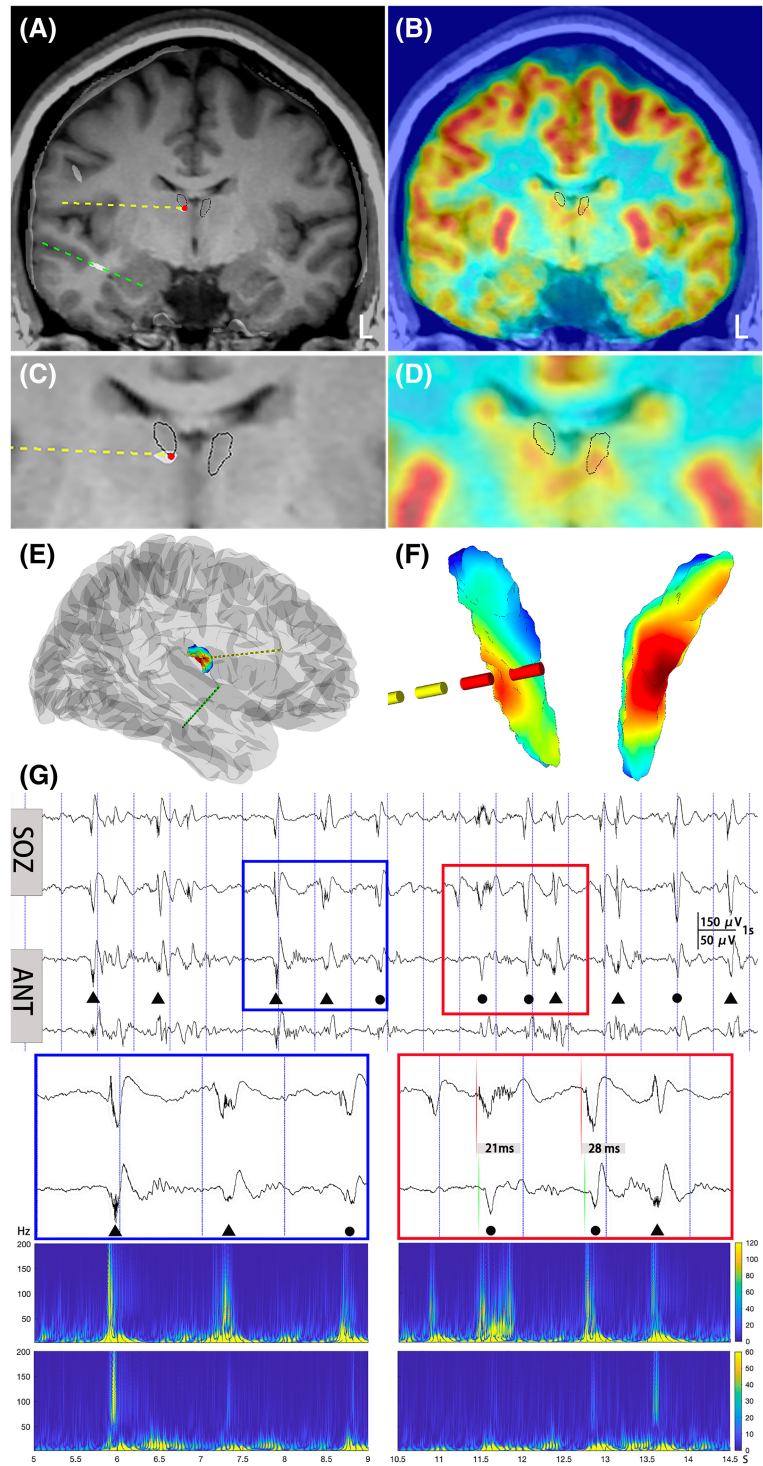


Figure 3. Reconstruction of the depth electrodes and recording of interictal activities in the ANT and SOZ in a patient with TLE (patient 13). (A, C, E) Reconstruction in 2D and 3D views of the depth electrodes in the ANT (yellow) and SOZ (green); the red points are the contacts in the ANT. (B, D, F) PET-MRI and 3D view of the ANT; the red contacts are located in the ANT region. (G) Interictal activities of the SOZ and ANT; HFO (black triangle) and synchronous spikes (black circle) were recorded in the ANT. The time interval of the beginning of the synchronous spike between the SOZ (red vertical line) and ANT (green vertical line) was 21 and 28 msec, respectively (zoomed red boxes). The bottom of this image is the time–frequency analysis of the interictal activities in the SOZ and ANT corresponding to the blue and red boxes. L, left.

was no correlation ($p > 0.05$) between the degree of nRCV of the ANT and the discharge of the ANT. In patients with hypometabolism in the ANT ipsilateral to the SOZ, the spike is recorded in seven patients (6 TLE

vs. 1 ETLE). The slow-wave activity was recorded in six patients (1 TLE vs. 5 ETLE).

Two patterns of spikes were recorded in the ANT of the 10 patients with spikes, the synchronous spike was

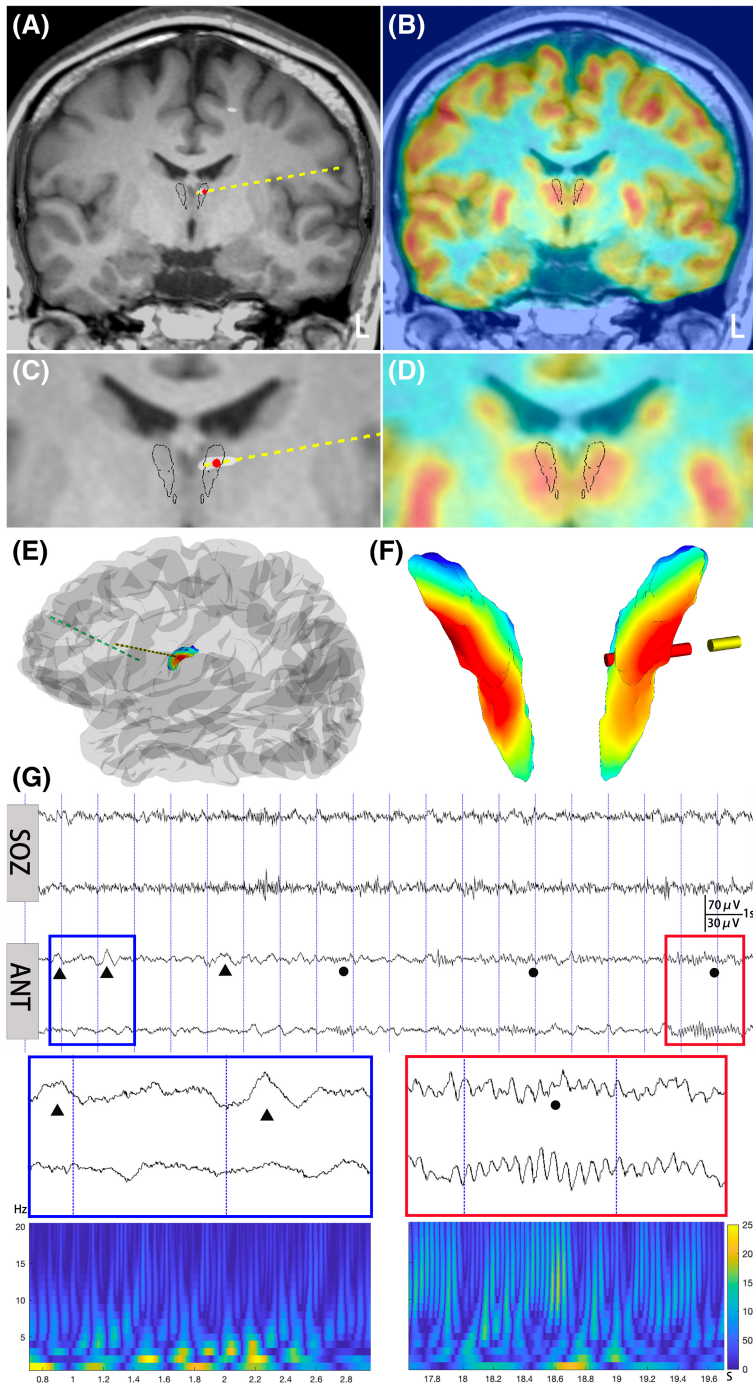


Figure 4. Reconstruction of the depth electrodes and recording of interictal activities in the ANT and SOZ in a patient with ETLE (patient 18). (A, C, E) Reconstruction (in 2D and 3D views) of the depth electrodes in the ANT (yellow) and SOZ (green); the red points are the contacts in the ANT. (B, D, F) PET-MRI and 3D view of the ANT; the red contacts are located in the ANT. (G) Interictal activities of the SOZ and ANT; slow-wave (black triangle) and α -rhythmic activities (black circle) were recorded in the ANT. The bottom of this image is the time–frequency analysis of the interictal activities in the ANT corresponding to the blue and red boxes. L, left.

recorded in eight patients (7 of 8 patients had TLE), and the independent spike was recorded in three patients (two patients had ETLE). Two patterns of spikes were noted in one patient with TLE (Patient 17, Fig. 5). The time interval between the beginning of the synchronous spike in SOZ and ANT was approximately 20–30 msec (Table 2).

Ictal activities of the ANT

One patient was excluded from the analysis of ictal discharge because the electrode in the ANT was implanted contralateral to the EZ (Patient 12). A total of 150 epileptic seizures (3–22 seizures for each patient, with an average of 8.3 ± 4.9 times) were recorded in 18 patients. The

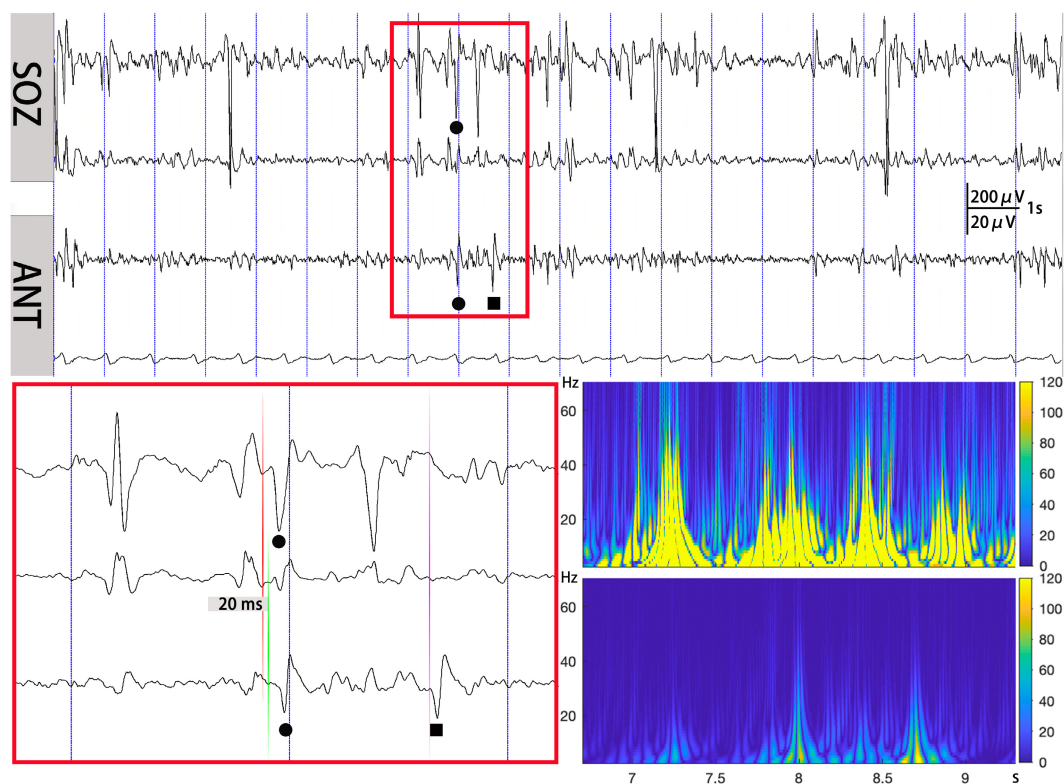


Figure 5. Two patterns of the spike in the ANT. Interictal activities of the SOZ and ANT of patient 17; synchronous (black circle) and independent (black square) spikes were recorded. The time interval of the beginning of the S-spike between the SOZ (red vertical line) and ANT (green vertical line) was 20 msec; an independent spike (purple vertical line) in the ANT was recorded (zoomed red box). Image reconstruction revealed that the second contact in the ANT was close to the thalamostriate veins, and the discharge rhythm was synchronous with the heart rate.

ictal epileptic activity of the ANT was recorded in 45 of 54 (83.3%) selected seizures. Three patients were recorded as ‘None’, which means that the ANT did not participate in seizures. Patients 3 and 16 showed no obvious electrographic changes in the ANT during seizures, and the clinical signs preceded the EEG alteration in patient 15. The seizure onset activities of the ANT were classified into three types: LVFA in eight patients (four TLE vs. four ELTE), RS in four patients (four TLE vs. zero ELTE) and theta discharge in three patients (one TLE vs. two ELTE). Typical examples of different seizure types of ANT are shown in Figure 6. There was no significant difference in ANT seizure types between patients with TLE and those with ETLE. In patients with hypometabolism in the ANT ipsilateral to the SOZ, LVFA was recorded in six patients (3 TLE vs. 3 ETLE), RS was recorded in four patients with TLE, and theta discharge was recorded in one patient with ETLE (Fig. 2).

The interval of seizure onset between the SOZ and ANT was difficult to calculate precisely visually, although it was confirmed that seizure onset in the ANT did not precede SOZ seizures in the seizures we studied. Notably,

two patterns were recorded in these seizures: immediate (seizure onset between the ANT and SOZ almost simultaneously) and delayed patterns (seizure onset between the ANT and SOZ showed a longer interval, at least >1 s) (Fig. 6A and B). There was no significant difference ($p > 0.05$) in ictal interval patterns between the TLE and ETLE groups.

Discussion

In this study, we investigated metabolic anomalies and interictal and ictal discharges of ANT in patients with TLE or ETLE. We attempted to demonstrate the role of ANT in the cortical–subcortical epileptic network, which will contribute to a better understanding of ANT-DBS mechanisms.

Metabolic anomalies in the ANT and SEEG findings

The metabolic differences between the bilateral ANT’s upon visual evaluation were significant in the TLE group.

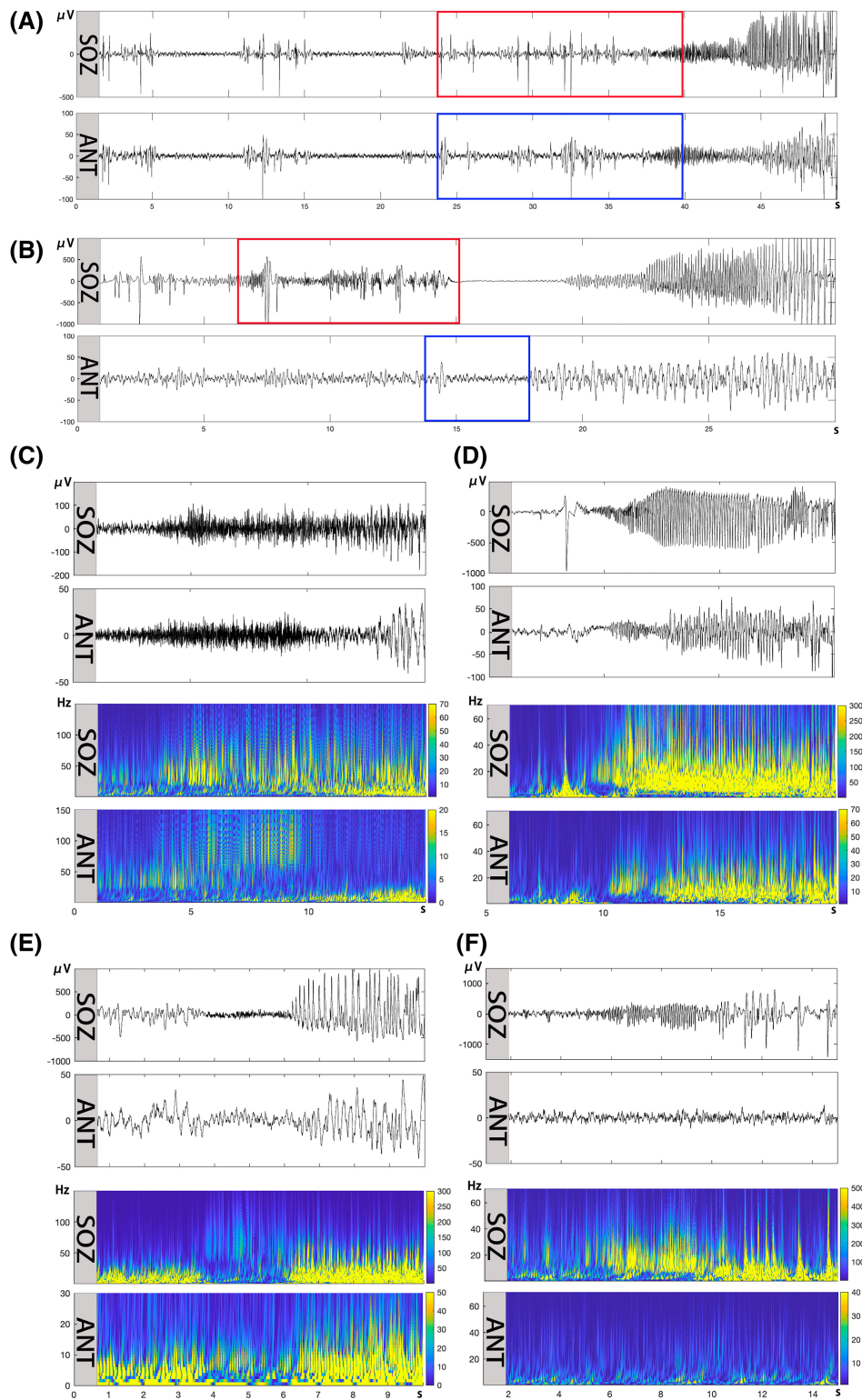


Figure 6. Two patterns of the ictal interval between SOZ and ANT, and examples of the seizure onset types of the ANT. (A) Immediate pattern: the seizure onset between the SOZ (red boxes) and ANT (blue boxes) almost simultaneously. (B) Delayed patterns: the seizure onset between the SOZ (red boxes) and ANT (blue boxes) shows a longer interval, about 8 sec. Examples of seizure onset types of the ANT and their time–frequency analysis: LVFA (C), RS (D) and theta (E). (F) There was no obvious evolution of activities in the ANT during ictal evolution in the SOZ.

Furthermore, we compared the AAI of the ANT between the TLE and ETLE groups. Consistent with visual analysis, ANT asymmetry was significant in patients with TLE. In line with the previous report, we also speculate that the ANT is susceptible to the ipsilateral EZ of the temporal lobe.³⁵ In other words, the ANT was more involved in the interictal epileptic network in TLE than in ETLE. Electrophysiological data from the SEEG recordings further confirmed this assumption.

In the study by Pizzo *et al.*, the thalamus was involved in focal seizures in the majority of patients, and they speculated that the participation of the thalamus might be in all focal epilepsies having nothing to do with localization or aetiology.⁶ Similarly, in our study, ictal discharge of the ANT was recorded in most patients, which indicates that the ANT is involved in seizure propagation. However, the temporal interval of seizure onset between SOZ and ANT varied significantly in different patients, similar to a previous study.³⁶ The reasons and influencing factors require further investigation. In contrast to ictal EEG with varied changes, a stable interictal EEG may provide a new perspective.

Interictal SEEG studies detected four types of waveforms in the interictal recordings of the ANT. Spike and HFO waveforms in the ANT were mainly recorded in patients with TLE, whereas slow-wave and α -rhythmic waveforms were recorded mainly in patients with ETLE. We believe that the spike and HFO waveforms in the ANT were epileptic discharges.^{16,18,37,38} The slow-wave and α -rhythmic waveforms tend to be considered as a physiological activity, although more research is needed to confirm this. We assumed that these different waveforms may reflect the differential epileptic excitability of the ANT in the cortico-subcortical epileptic network. In most patients with TLE, the reduced metabolism of the ANT, as well as the increased epileptic excitability, suggests a tight functional connection and pathological interaction between the epileptogenic zone and ANT.

In a previous study, ANT thinning was observed in patients with TLE by high-resolution MRI.³⁹ The authors suggested that the loss of volume was related to seizure propagation from the SOZ to the thalamus, leading to neuronal loss in the ANT. Another study observed a reduction in synapse density in the ANT, together with increased levels of gliosis in a TLE model in macaques.¹² Based on previous studies, we speculated that ANT hypometabolism is related to these cellular reorganizations, which is secondary to the abnormal functional connection between the temporal lobe and ANT.

Even in the patients with TLE, the previous study reported that the frequency of interictal epileptiform discharges in the ANT was correlated with that in surface EEG.¹⁶ It is usually difficult to clarify the temporal

relationship between epileptic discharges in the SOZ and ANT.^{16,37} However, the use of SEEG in the present study allowed us to analyse spike activity in the SOZ and ANT. We discovered two patterns of spike activity in ANT: synchronous and independent spikes. In the first pattern, the time interval of the spike between the SOZ and ANT was approximately 20–30 msec, which may imply the propagation of interictal discharges from the SOZ to the ANT. The functional and anatomical connections between the ANT and hippocampus have been verified in several previous studies.^{39–41} According to our previous study, the bidirectional cortico-cortical evoked potential (CCEP) connection between the ANT and hippocampus was recorded in similar patients.⁴² Furthermore, in this study, we provide additional evidence for abnormal connectivity of the ANT and hippocampus in patients with TLE. Abnormal connectivity might also be related to the hypometabolism of the ANT. In addition, the independent discharges recorded in the ANT also indicate the abnormal excitability of the ANT. Another interesting finding is the HFOs recorded in the ANT, which were also detected using the implanted DBS electrodes.³⁷ As we know, HFO is usually seen as a specific epileptogenic activity in the epileptogenic zone.^{43,44} Therefore, these data collectively indicate that the ANT is a crucial node of the cortical–subcortical epileptic network during the interictal stage.

Additionally, various types of seizure onset in the thalamus have been studied and reported.^{6,17,37,38,45} In concordance with previous research, similar seizure onset types of ANT were also recorded in our studies, such as LVFA, RS, and theta discharge. Due to the limited study cohort, a difference in seizure onset types of the ANT between TLE and ETLE was not found.

Metabolic anomalies in the ANT and surgical outcomes

In the present study, we found that patients with hypometabolism in the ANT ipsilateral to the SOZ had better surgical outcomes. A previous study also reported that hypometabolism in the thalamus ipsilateral to the SOZ was associated with better surgical outcomes than contralateral thalamic hypometabolism.⁴⁶ Although reverse ANT asymmetry is less common in patients with epilepsy,^{46,47} these patients with reverse ANT asymmetry appear to have worse surgical outcomes.

Novel understandings of ANT-DBS

Different from the intervention of responsive neurostimulation in the ictal stage of seizure,^{48,49} ANT-DBS may perform chronic modulation in the interictal stage to

decrease the excitability of the epileptic network. In previous studies, the close relationship between ANT and the temporal lobe has been confirmed from the perspectives of functional anatomical connections, pathological biopsy, ictal EEG and electrical stimulation.^{7,12,16,35,42} In our study, further evidence of interictal discharges and decreased metabolism in the ipsilateral ANT of the epileptic temporal lobe was provided. This new evidence indicates that the ANT not only acts as an important node in the cortical-subcortical epileptic network during the interictal stage, especially for patients with TLE. Based on this evidence, we can further understand the antiepileptic mechanisms of ANT-DBS. In addition to the indirect inhibition of local field potentials and epileptic discharges in the hippocampus we have reported,⁴² we speculate that the direct interference of the interictal epileptic discharges that either propagated from the SOZ to the ANT or generated in the ANT might be a potential antiepileptic mechanism of ANT-DBS. As a result, we infer that effective stimulation of the ANT can weaken the pathological connection between the EZ and the ANT.

Limitations

This study was based on clinical data and had several limitations that need to be considered. First, PET data were compared between the ipsilateral and contralateral ANT, rather than being compared with the ANT of healthy individuals. Second, although the statistics showed significance in different group comparisons, the small study cohort limited the statistical power of some experiments. Third, it is difficult to record all thalamus nuclei that participated in the seizures because of the limitation of the spatial sampling of the SEEG.

Acknowledgements

The authors would like to thank Xiaoxia Zhou, Yuanyuan Piao, Liu He and Xiumei Wang for their assistance with the collection of EEG data and follow-up information. The authors are enormously indebted to the patients who participated in this study as well as the nursing and physician staff at each facility.

Conflict of Interest

The authors declared no conflict of interest.

Author Contributions

H.Y., X.Y.W., T.Y. and L.K.R. contributed to the conception and design of the study. H.Y., X.Y.W., T.Y., L.K.R.,

Y.P.W., C.P.X. and W.S. contributed to the analysis of data. X.H.Z., D.Y.N., L.Q., C.P.X. and W.S. contributed to the data acquisition. H.Y., X.Y.W., T.Y., L.K.R., Y.P.W. and C.P.X. contributed to drafting the manuscript, figures and interpreting the results. All authors reviewed and revised the manuscript for intellectual content.

References

1. Theodore WH, Fisher RS. Brain stimulation for epilepsy. *Lancet Neurol.* 2004;3(2):111-118.
2. Fisher RS, Velasco AL. Electrical brain stimulation for epilepsy. *Nat Rev Neurol.* 2014;10(5):261-270.
3. Keller SS, Richardson MP, Schoene-Bake JC, et al. Thalamotemporal alteration and postoperative seizures in temporal lobe epilepsy. *Ann Neurol.* 2015;77(5):760-774.
4. Feng L, Motelow JE, Ma C, et al. Seizures and sleep in the thalamus: focal limbic seizures show divergent activity patterns in different thalamic nuclei. *J Neurosci.* 2017;37(47):11441-11454.
5. He X, Doucet GE, Pustina D, Sperling MR, Sharan AD, Tracy JJ. Presurgical thalamic "hubness" predicts surgical outcome in temporal lobe epilepsy. *Neurology.* 2017;88(24):2285-2293.
6. Pizzo F, Roehri N, Giusiano B, et al. The ictal signature of thalamus and basal ganglia in focal epilepsy: a SEEG study. *Neurology.* 2021;96(2):e280-e293.
7. Papez JW. A proposed mechanism of emotion. *Arch Neurol Psychiatry.* 1937;38(4):725-743.
8. Fisher R, Salanova V, Witt T, et al. Electrical stimulation of the anterior nucleus of thalamus for treatment of refractory epilepsy. *Epilepsia.* 2010;51(5):899-908.
9. Salanova V, Witt T, Worth R, et al. Long-term efficacy and safety of thalamic stimulation for drug-resistant partial epilepsy. *Neurology.* 2015;84(10):1017-1025.
10. Udupa K, Chen R. The mechanisms of action of deep brain stimulation and ideas for the future development. *Prog Neurobiol.* 2015;133:27-49.
11. Gastaut H, Broughton RJ. *Epileptic Seizures; Clinical and Electrographic Features, Diagnosis and Treatment.* Thomas; 1972.
12. Sherdil A, Coizet V, Pernet-Gallay K, David O, Chabardes S, Pierrat B. Implication of anterior nucleus of the thalamus in mesial temporal lobe seizures. *Neuroscience.* 2019;418:279-290.
13. Devergnas A, Pierrat B, Prabhu S, et al. The subcortical hidden side of focal motor seizures: evidence from micro-recordings and local field potentials. *Brain.* 2012;135(Pt 7):2263-2276.
14. Chassoux F, Artiges E, Semah F, et al. Determinants of brain metabolism changes in mesial temporal lobe epilepsy. *Epilepsia.* 2016;57(6):907-919.
15. Wyckhuys T, Geerts PJ, Raedt R, Vonck K, Wadman W, Boon P. Deep brain stimulation for epilepsy: knowledge

- gained from experimental animal models. *Acta Neurol Belg.* 2009;109(2):63-80.
16. Sweeney-Reed CM, Lee H, Rampp S, et al. Thalamic interictal epileptiform discharges in deep brain stimulated epilepsy patients. *J Neurol.* 2016;263(10):2120-2126.
 17. Pizarro D, Ilyas A, Chaitanya G, et al. Spectral organization of focal seizures within the thalamotemporal network. *Ann Clin Transl Neurol.* 2019;6(9):1836-1848.
 18. Osorio I, Frei MG, Lozano AM, Wennberg R. Subcortical (thalamic) automated seizure detection: a new option for contingent therapy delivery. *Epilepsia.* 2015;56(10):e156-e160.
 19. Widjaja E, Shamma A, Vali R, et al. FDG-PET and magnetoencephalography in presurgical workup of children with localization-related nonlesional epilepsy. *Epilepsia.* 2013;54(4):691-699.
 20. Sidhu MK, Duncan JS, Sander JW. Neuroimaging in epilepsy. *Curr Opin Neurol.* 2018;31(4):371-378.
 21. Fisher RS, Cross JH, French JA, et al. Operational classification of seizure types by the international league against epilepsy: position paper of the ILAE Commission for Classification and Terminology. *Epilepsia.* 2017;58(4):522-530.
 22. Qin C, Tan Z, Pan Y, et al. Automatic and precise localization and cortical labeling of subdural and depth intracranial electrodes. *Front Neuroinform.* 2017;11:10.
 23. Mottonen T, Katisko J, Haapasalo J, et al. Defining the anterior nucleus of the thalamus (ANT) as a deep brain stimulation target in refractory epilepsy: delineation using 3 T MRI and intraoperative microelectrode recording. *Neuroimage Clin.* 2015;7:823-829.
 24. Buentjen L, Kopitzki K, Schmitt FC, et al. Direct targeting of the thalamic anteroventral nucleus for deep brain stimulation by T1-weighted magnetic resonance imaging at 3 T. *Stereotact Funct Neurosurg.* 2014;92(1):25-30.
 25. Alkonyi B, Juhasz C, Muzik O, et al. Quantitative brain surface mapping of an electrophysiologic/metabolic mismatch in human neocortical epilepsy. *Epilepsy Res.* 2009;87(1):77-87.
 26. Lopez-Gonzalez FJ, Silva-Rodriguez J, Paredes-Pacheco J, et al. Intensity normalization methods in brain FDG-PET quantification. *Neuroimage.* 2020;222:117229.
 27. Goutal S, Tournier N, Guillemier M, et al. Comparative test-retest variability of outcome parameters derived from brain [18F]FDG PET studies in non-human primates. *PLoS One.* 2020;15(10):e0240228.
 28. Steriade M, Glenn LL. Neocortical and caudate projections of intralaminar thalamic neurons and their synaptic excitation from midbrain reticular core. *J Neurophysiol.* 1982;48(2):352-371.
 29. Briggs F, Usrey WM. A fast, reciprocal pathway between the lateral geniculate nucleus and visual cortex in the macaque monkey. *J Neurosci.* 2007;27(20):5431-5436.
 30. Robinson PA, Rennie CJ, Rowe DL, O'Connor SC. Estimation of multiscale neurophysiologic parameters by electroencephalographic means. *Hum Brain Mapp.* 2004;23(1):53-72.
 31. Roberts JA, Robinson PA. Modeling absence seizure dynamics: implications for basic mechanisms and measurement of thalamocortical and corticothalamic latencies. *J Theor Biol.* 2008;253(1):189-201.
 32. Salami M, Itami C, Tsumoto T, Kimura F. Change of conduction velocity by regional myelination yields constant latency irrespective of distance between thalamus and cortex. *Proc Natl Acad Sci U S A.* 2003;100(10):6174-6179.
 33. Lagarde S, Buzori S, Trebuchon A, et al. The repertoire of seizure onset patterns in human focal epilepsies: determinants and prognostic values. *Epilepsia.* 2019;60(1):85-95.
 34. Wieser HG, Blume WT, Fish D, et al. ILAE commission report. Proposal for a new classification of outcome with respect to epileptic seizures following epilepsy surgery. *Epilepsia.* 2001;42(2):282-286.
 35. Morgan VL, Rogers BP, Abou-Khalil B. Segmentation of the thalamus based on BOLD frequencies affected in temporal lobe epilepsy. *Epilepsia.* 2015;56(11):1819-1827.
 36. Pizarro D, Ilyas A, Toth E, et al. Automated detection of mesial temporal and temporoparietal seizures in the anterior thalamic nucleus. *Epilepsy Res.* 2018;146:17-20.
 37. Rektor I, Dolezalova I, Chrastina J, et al. High-frequency oscillations in the human anterior nucleus of the thalamus. *Brain Stimul.* 2016;9(4):629-631.
 38. Hodaie M, Wennberg RA, Dostrovsky JO, Lozano AM. Chronic anterior thalamus stimulation for intractable epilepsy. *Epilepsia.* 2002;43(6):603-608.
 39. Mueller SG, Laxer KD, Barakos J, et al. Involvement of the thalamocortical network in TLE with and without mesiotemporal sclerosis. *Epilepsia.* 2010;51(8):1436-1445.
 40. Aggleton JP, O'Mara SM, Vann SD, Wright NF, Tsanov M, Erichsen JT. Hippocampal-anterior thalamic pathways for memory: uncovering a network of direct and indirect actions. *Eur J Neurosci.* 2010;31(12):2292-2307.
 41. Middlebrooks EH, Grewal SS, Stead M, Lundstrom BN, Worrell GA, Van Gompel JJ. Differences in functional connectivity profiles as a predictor of response to anterior thalamic nucleus deep brain stimulation for epilepsy: a hypothesis for the mechanism of action and a potential biomarker for outcomes. *Neurosurg Focus.* 2018;45(2):E7.
 42. Yu T, Wang X, Li Y, et al. High-frequency stimulation of anterior nucleus of thalamus desynchronizes epileptic network in humans. *Brain.* 2018;141(9):2631-2643.
 43. Chen Z, Maturana MI, Burkitt AN, Cook MJ, Grayden DB. High-frequency oscillations in epilepsy: what have we learned and what needs to be addressed. *Neurology.* 2021;96(9):439-448.

44. Sharifshazileh M, Burelo K, Sarnthein J, Indiveri G. An electronic neuromorphic system for real-time detection of high frequency oscillations (HFO) in intracranial EEG. *Nat Commun.* 2021;12(1):3095.
45. Rosenberg DS, Mauguire F, Demarquay G, et al. Involvement of medial pulvinar thalamic nucleus in human temporal lobe seizures. *Epilepsia.* 2006;47(1):98-107.
46. Newberg AB, Alavi A, Berlin J, Mozley PD, O'Connor M, Sperling M. Ipsilateral and contralateral thalamic hypometabolism as a predictor of outcome after temporal lobectomy for seizures. *J Nucl Med.* 2000;41(12):1964-1968.
47. Choi JY, Kim SJ, Hong SB, et al. Extratemporal hypometabolism on FDG PET in temporal lobe epilepsy as a predictor of seizure outcome after temporal lobectomy. *Eur J Nucl Med Mol Imaging.* 2003;30(4):581-587.
48. Kossoff EH, Ritzl EK, Politsky JM, et al. Effect of an external responsive neurostimulator on seizures and electrographic discharges during subdural electrode monitoring. *Epilepsia.* 2004;45(12):1560-1567.
49. Stacey WC, Litt B. Technology insight: neuroengineering and epilepsy-designing devices for seizure control. *Nat Clin Pract Neurol.* 2008;4(4):190-201.